NANO LETTERS

2007
Vol. 7, No. 5
1406−1412

Facile Electrochemical Characterization of Core/Shell Nanoparticles. Ag Core/Ag_2O Shell Structures

Jalal Ghilane, Fu-Ren F. Fan, and Allen J. Bard*

Department of Chemistry and Biochemistry, The University of Texas at Austin, Austin, Texas 78712

Nicholas Dunwoody

NUCRYST Pharmaceuticals Inc., Wakefield, Massachusetts 01880

Received February 2, 2007; Revised Manuscript Received March 12, 2007

ABSTRACT

We report in this paper a facile approach for the formation and electrochemical characterization of silver–silver oxide core–shell nanoparticles (NPs). Thus, thermal treatment at temperatures between 200 and 360 °C of Ag NP, in the gas phase or in an organic solvent, has been used to achieve the formation Ag@Ag_2O NP. The evidence of formation of such a core–shell structure was obtained by cyclic voltammetry using a Nafion modified electrode (where Nafion containing carbon particles is used as the matrix to encapsulate the core–shell NP). Initial positive scans measure free Ag. Initial negative scans measure Ag_2O, with the following positive scan, compared to the initial one, providing a measure of "trapped" or core Ag. The results presented demonstrate the utility of this approach in characterizing core–shell structures, like Ag@Ag_2O, which could be extended to other core–shell forms, such as bimetallic core–shell NP.

We describe here a simple electrochemical approach to determine the composition of metallic core/shell nanoparticles (NPs). Over the past decade metal nanostructures have been extensively studied because differences between their optical and electronic properties and those of the corresponding bulk material have been used in applications such as catalysis, electronics, photography, optics, information storage, biological and chemical sensing, and surface-enhanced Raman scattering (SERS).[1−5] Recently, there have been several reports on the formation of core−shell NPs. Such structures often show a combination of the properties of the two (or more) materials involved, where the shell determines the surface properties of the particles, while the core is completely encapsulated by the shell.[6] Coated nanomaterials provide a very high surface area and possess chemical and physical properties that are distinct from those of both bulk phase and individual molecules.[7] Typically the growth of a core−shell structure can be accomplished by the successive reduction of one metal ion over the core of the other metal. For example, Turkevich and Kim had used the successive reduction method to fabricate gold-layered Pd NP.[8] More recently, many reports on the preparation of core−shell NP of Au−Ag,[9,10] Au−Pd,[11,12] Au−Pt,[13,14] and their combinations have appeared based on this growth technique.[15] The formation of core−shell with semiconductors as the shell (e.g., Co−CdSe) has also been reported.[16] However, core−shells with a metal core and its oxide as the shell have not been as widely investigated, although oxide films on active metal particles are a frequent occurrence. For example, Hyeon and Lee showed the formation of NiO-coated Ni NPs, using thermal decomposition of Ni−alkylamine following by oxidation in air.[17]

In the past, NPs or core−shell NPs have been widely characterized using microscopic techniques such as transmission electron microscopy (TEM) and scanning electron microscopy (SEM), as well as X-ray photoelectron spectroscopy (XPS), X-ray diffraction (XRD), and optical technique such as UV−vis absorption spectroscopy.[18]

This work involves the formation of a Ag_2O shell on a Ag core, represented as Ag@Ag_2O, using thermal treatment of Ag NPs, and their facile characterization using electrochemistry (cyclic voltammetry). The electrochemical characterization is based on the examination of the core−shell NP on a gold electrode in a cast Nafion film containing carbon as an electronically conductive matrix. We have been using such films to study mixtures of metal NPs with particles of their oxides and other compounds; the details of this work will be reported elsewhere.[19] Nafion provides a convenient chemically inert and ionically conductive matrix for electrochemical studies of NPs and is a useful complement to the optical techniques for their characterization.

10.1021/nl070268p CCC: $37.00
Published on Web 04/03/2007

Scheme 1. Formation of $Ag@Ag_2O$ NPs Using Thermal Treatment

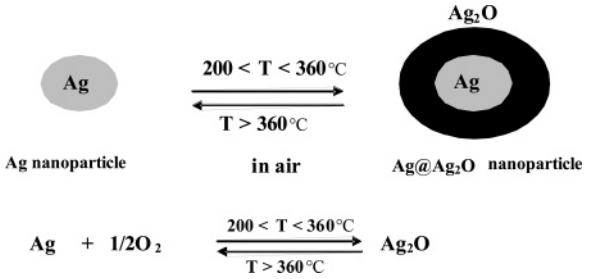

Experimental Section. In this work $Ag@Ag_2O$ NPs were prepared using thermal treatment. Typically commercial Ag NP powder (Aldrich, diameter less than 100 nm) was heated in a furnace in air at 260 °C for 6 h. This temperature was chosen to avoid the total decomposition of Ag_2O, which begins at about 360 °C.[20] Then, the sample was removed from the furnace and allowed cool in air to room temperature. This sample is labeled powder 1. Alternatively commercial Ag NPs were dispersed in propylene carbonate with stirring and heated to 220 °C for 8 h. The precipitate that formed was filtered and washed several times with deionized DI water to remove residual solvent (powder 2). Thus thermal treatment of Ag NPs, at temperatures higher than 200 °C, but less than 360 °C to avoid decomposition of silver oxide, leads to the formation of a thin layer of silver oxide on the silver NPs to form Ag@Ag2O NPs as illustrated in Scheme 1.

The preparation of solution $Ag@Ag_2O$ NP Nafion film was achieved as follows. First, 1 mL of Nafion polymer solution, obtained as a 5% (w/w) alcoholic solution (Alfa-Aesar) (pH = 2), was mixed with 0.70 g of graphite powder (~10 μm particle size, measured by SEM), where graphite is used to enhance the electronic conductivity of the film. This solution was diluted with 40 mL of MeOH, yielding a solution of pH 5.5. The pH of the solution was adjusted to about 7 by adding 0.1 M NaOH, followed by the addition of MeOH to obtain a total volume of 50 mL. A 10 mg sample of powder 1 or 2 was added to the solution and sonicated for 30 min to form a suspension. For the immobilization of the $Ag@Ag_2O$ NP/C/Nafion suspension on an electrode, a gold disk (0.2 cm diameter) imbedded in Teflon (0.5 cm diameter) was used as the working electrode. Before film preparation, the gold disk was polished with 0.3 μm alumina and fixed horizontally facing up. A 10.0 μL drop of the $Ag@Ag_2O$/C/Nafion suspension was placed on the gold electrode with a micropipet. The drop covered both the gold and at least some of the Teflon surface but did not leak down the sides of the electrode. The electrode was covered to prevent exposure to light, and the solvent, MeOH, was allowed to evaporate at room temperature (requiring 20−30 min). The thickness of the resulting film, as measured by scanning electrochemical microscopy (SECM) in solution and SEM in vacuum, was about 50 μm. Because the film is electronically conductive, even parts not in direct contact with the gold were electrochemically addressable.

Electrochemical measurements were performed with a CHI model 660 electrochemical workstation (CH Instruments, Austin, TX). For cyclic voltammetry experiments at a scan rate of 0.1V/s, a conventional three-compartment sealed glass cell was used: reference electrode, Pt/PPy quasi-reference electrode; counter electrode, graphite; working electrode, modified gold disk with Nafion−$Ag@Ag_2O$ film. In our previous work, we demonstrated the stability of Pt/PPy as a quasi-reference electrode, with a potential under these conditions of −0.189 V vs SCE.[21] This electrode has several advantages, like the absence of a liquid/liquid junction and problems related to the contamination of the test solution by Cl^- or Ag^+ when a reference electrode like Ag/AgCl is used.[21]

The electrochemical measurements were carried out in sodium citrate buffer solution. The solution was made by dissolving sodium citrate (Aldrich) to produce a 0.01 M solution in DI water and adjusting the pH to 6.8 by adding citric acid (Aldrich, 99.5%). Citrate instead of phosphate-buffered saline or Tris buffer solution was used because of its very low tendency to interact with Ag^+ at room temperature (25 ± 0.5 °C) (at higher temperatures, however, citrate will reduce Ag^+ in solution to Ag). To this solution $NaClO_4$ at 0.1 M was added as supporting electrolyte. All experiments were conducted after degassing and under an argon atmosphere at room temperature.

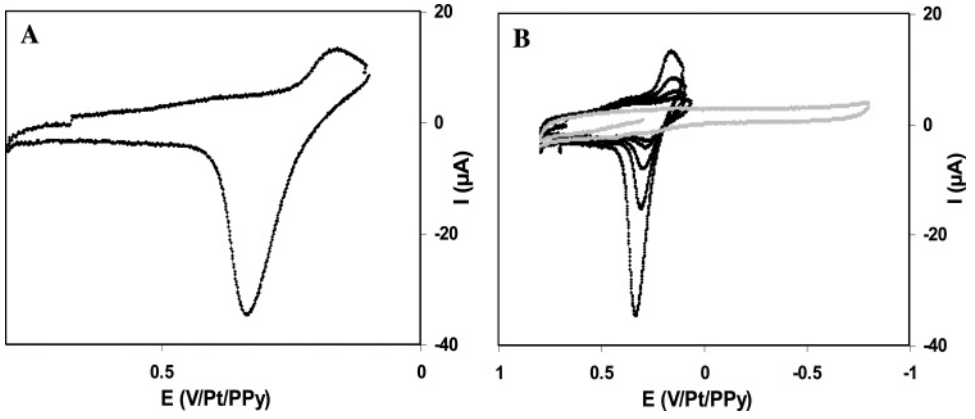

Figure 1. Cyclic voltammetry of Ag incorporated in Nafion film on a gold electrode in sodium citrate buffer 0.1 M $NaClO_4$: (A) the first scan; (B) successive scans for the same film, where the gray line is the last scan (after seven scans). Scan rate was 0.1 V/s.

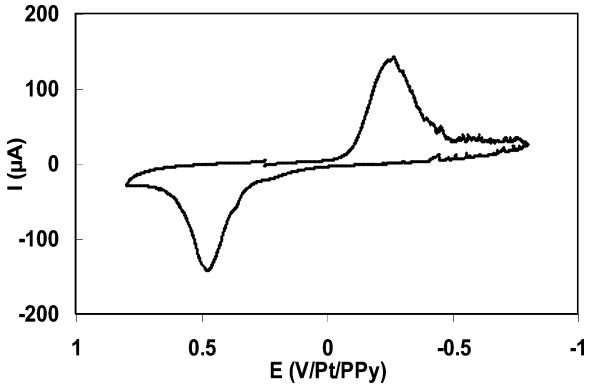

Figure 2. Cyclic voltammetry of Ag_2O incorporated in Nafion/C film on a gold electrode in sodium citrate buffer−0.1 M $NaClO_4$ as supporting electrolyte. Scan rate was 0.1 V/s.

Results and Discussion. (A) Electrochemistry of Ag NP Immobilized in Nafion. As a preliminary experiment the electrochemical behavior of a film of untreated silver Ag NPs incorporated in Nafion onto a gold electrode was studied. Figure 1A shows the cyclic voltammograms (CVs) starting from 0.1 V vs Pt/PPy and scanning in the positive direction.

As expected, the curve shows oxidation peaks at 0.4 V corresponding to the oxidation of Ag to Ag^+ and, on the reverse scan, reduction peaks at 0.15 V corresponding to the reduction of Ag^+ to Ag. With successive scans there is a decrease in both the oxidation and reduction peaks because of the diffusion of Ag^+, formed in the oxidation process, into the solution. This result suggests that Ag^+ is not strongly immobilized into the Nafion film. This observation was confirmed by CVs study of $AgNO_3$ incorporated in Nafion film and show lower recovery of Ag^+. After 10 cycles no electroactive species, neither Ag nor Ag^+, remained in the film as shown in Figure 1B (gray line).

The same experiment was carried using untreated Ag_2O particles (from Aldrich) incorporated in Nafion (see Figure 2). The CV shows reduction peaks at −0.3 V/Pt/PPy corresponding to reduction of Ag_2O to Ag followed by stripping peaks (Ag to Ag^+) at 0.4 V/Pt/PPy. The charge efficiency, CE, is defined as the ratio between the anodic (Q_a) and the cathodic charge (Q_c), $CE = Q_a/Q_c$. In the case of Ag_2O, the ratio between the anodic charge (Ag to Ag^+ after reduction) and the cathodic charge (Ag_2O to Ag) is $Q_a/Q_c = 0.9 \pm 0.08$.

(B) Electrochemical Characterization of Ag@Ag_2O Immobilized in Nafion. Successive scans of powders 1 and 2, in Nafion/C films on a gold electrode from 0.1 to 0.8 V vs Pt/PPy were carried out in the same solution as previously described. The film was first pretreated by cycling between 0.1 and 0.8 V to remove residual Ag NPs. After this treatment, a first CV scan to positive potentials from 0.1 V shows only a small anodic wave, then a reduction scan to −0.8 V, which reduces the surface (shell) Ag_2O, and finally scanning back to 0.8 V see Figure 3 with powder 1 (Figure 3A) and powder 2 (Figure 3B).

The first CV oxidative scan shown in Figure 3A starting from 0.1 V did not show significant peaks corresponding to the stripping of Ag. This observation demonstrates that the pretreatment removes any Ag NP in the film. When we continue scanning toward reduction, cathodic peaks appear at −0.3 V for reduction of Ag_2O to Ag. Following this reduction a large anodic peak at 0.4 V was observed due to the stripping of silver. A comparison between the anodic and cathodic peaks shows clearly that the anodic charge (Q_a) is much higher than the cathodic charge (Q_c), with a charge efficiency $CE = Q_a/Q_c \sim 8$, much larger than the value of 0.9 found with just Ag_2O NPs. A reasonable explanation of these results and the higher value of the CE obtained is that the Ag inside the Ag_2O shell is not oxidizable initially. Only after the Ag_2O shell is reduced is this exposed and then oxidized in an anodic scan. Thus, during the thermal treatment a Ag_2O layer is formed outside the silver NP. This oxide layer isolates the Ag core, probably by preventing electron transfer from the Ag. The electrochemical reduction process leads to removal (reduction) of the Ag_2O layer, and as consequence encapsulated Ag is now exposed and could be detected in an oxidation scan. Moreover, the high value of the CE suggests that only a thin layer of Ag_2O is sufficient to protect the core (reminiscent of other passivating oxide films). Untreated Ag NPs subjected to the same CV conditions after the electrochemical oxidative pretreatment showed no peaks (as in Figure 1B, gray line). The same result was obtained with powder 2 and the shape of the CV in

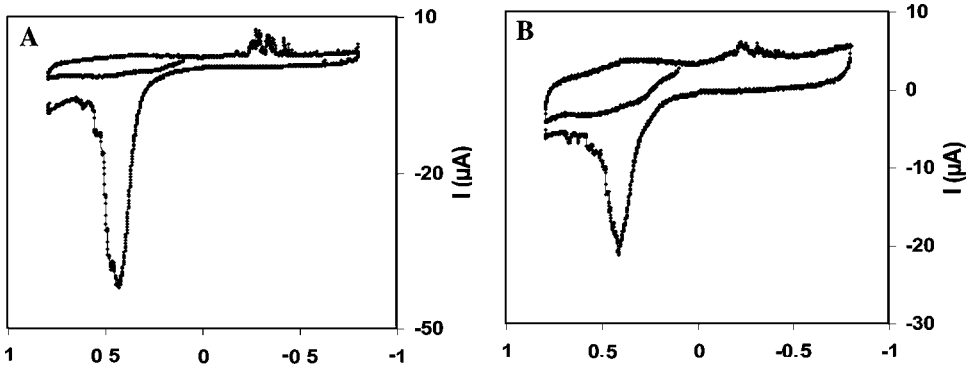

Figure 3. Cyclic voltammetry of Ag@Ag_2O incorporated on Nafion film above a gold electrode in sodium citrate buffer and 0.1 M $NaClO_4$ as supporting electrolyte: (A) Ag@Ag_2O NPs obtained after heating in furnace powder 1; (B) Ag@Ag_2O NPs obtained after heating in organic solvent powder 2. Scan rate was 0.1 V/s.

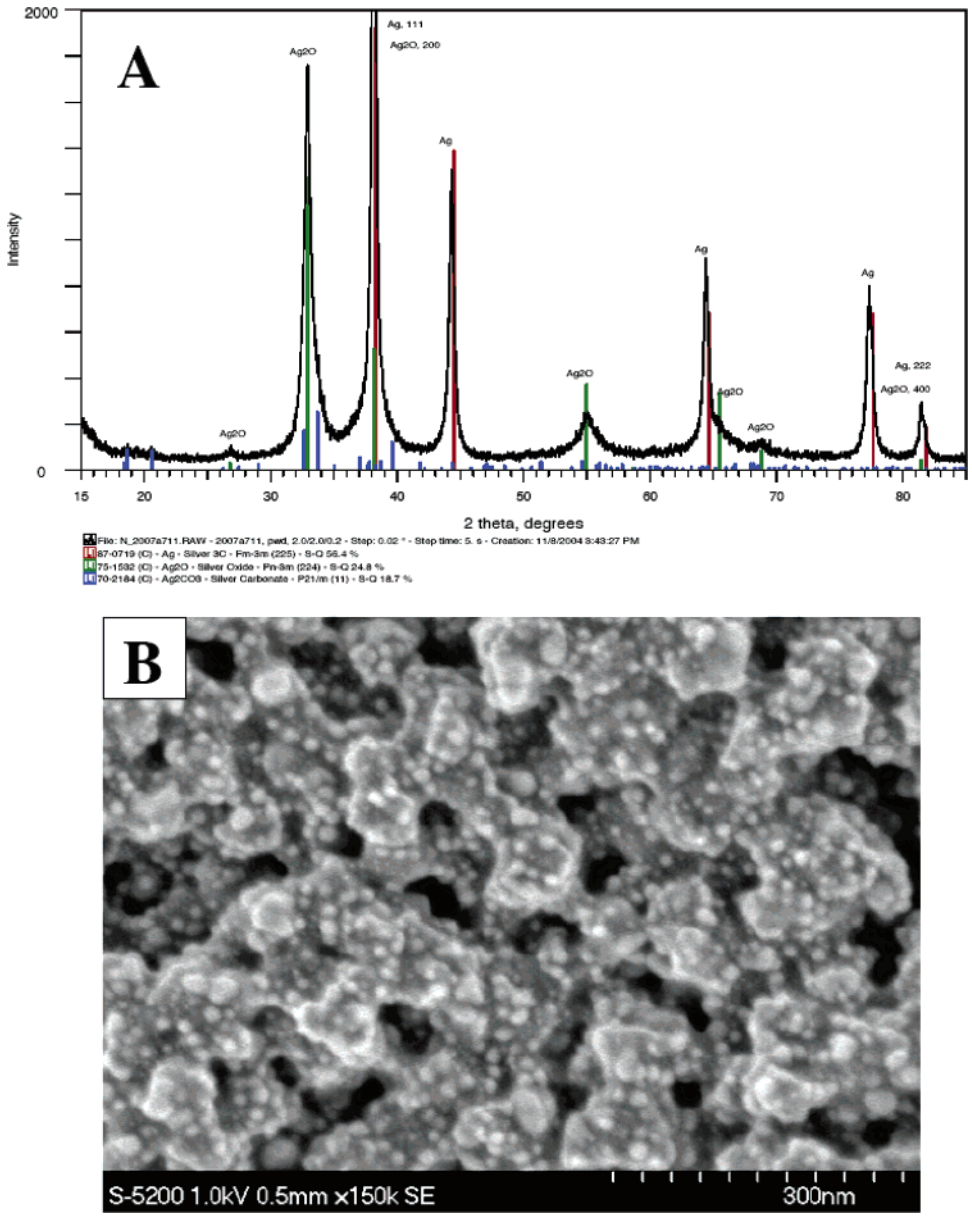

Figure 4. (A) XRD of nanocrystalline silver powder prepared by reactive sputtering of Ag onto a stainless steel substrate in the presence of oxygen. The vertical green lines mark the location of cubic silver oxide (Ag_2O) and red lines mark the location of the cubic silver (Ag) as is indicated on the figure. (B) High-resolution SEM micrograph of the silver nanocrystalline thin film. Each tick-mark represents 30 nm.

Figure 3B is similar to the CV of powder 1. Note that mixtures of Ag and Ag_2O NPs show the expected behavior that simply sums the responses of the two components.[19] All of these results suggest that the thermal treatment of Ag NPs produces Ag@Ag_2O and they can be examined by CV.

(C) Characterization of Commercial Ag Nanoparticle Preparation. The technique of electrochemical characterization of NPs was also used to characterize NPs produced by NUCRYST Pharmaceuticals Inc. (Wakefield, MA). These NPs are formed by reactive sputtering of Ag in oxygen and argon and contain both Ag and Ag_2O, either as a simple mixture or with some core−shell structures. Figure 4 shows the XRD spectra and the high-resolution SEM micrograph of this nanostructured silver, indicating that it is a mixture of nanocystalline silver(0) and Ag_2O aggregates with the crystals ranging in size from about 10 to 20 nm with an average size of 15 nm.

TEM images of aggregates of some silver NPs are shown in Figure 5, which reveals generally the core−shell structures of individual NPs (frame B). Diffraction fringes can also clearly be seen in some domains (frame C), indicating their crystalline structure. Energy dispersive spectrometry results (not shown) indicate that individual NPs contain only silver within its detection limit.

The electrochemical procedure used to study these NPs was the same as that described above, with a solution of 10 mg of NUCRYST NPs incorporated in Nafion−graphite used to cast a film onto a gold electrode. The CV recorded for this NUCRYST sample, with an oxidation scan first starting at 0.1 V, is shown in Figure 6.

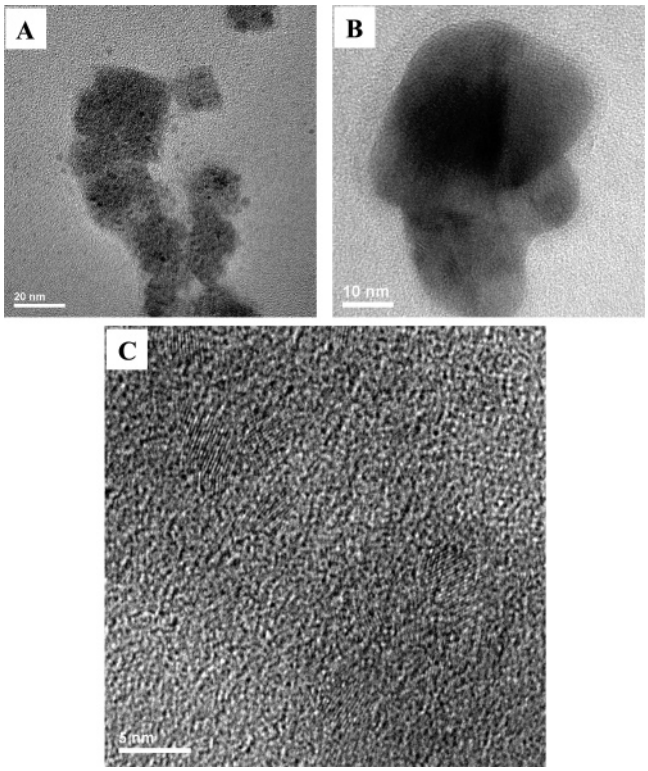

Figure 5. TEM images of silver NPs at increasing resolutions. The marks at the lower left bottom of the images represent (A) 20, (B) 10, and (C) 5 nm.

During the first oxidation scan, starting from 0.1 V, a small anodic peak at 0.4 V was observed corresponding to stripping of any free Ag NPs in the sample. The following reduction scan shows a cathodic peak at −0.3 V for the reduction of Ag_2O to Ag. Following this reduction, an anodic scan shows a large anodic peak at 0.4 V related to the stripping of Ag. A comparison between the cathodic and the second anodic peaks clearly shows that the anodic charge is much higher than the cathodic charge, with a CE of about 1.5. This large value to compare with the value 0.9 observed in the case of Ag_2O NPs demonstrates the presence of Ag inside the Ag_2O shell. Note that extensive studies on other samples as well as mixtures of Ag and Ag_2O free of core/shell structures do not show this behavior.[19] Thus the electrochemical characterization of NUCRYST NPs using cyclic voltammetry clearly demonstrates the presence of both Ag and Ag@Ag_2O NPs, which was not observed readily by spectroscopic techniques.

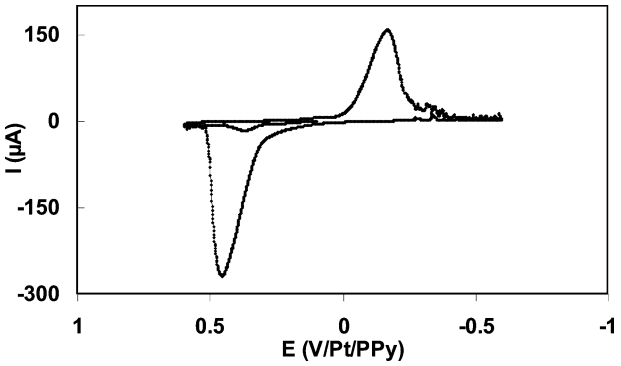

Figure 6. Cyclic voltammetry of NUCRYST NPs incorporated on Nafion film above a gold electrode in sodium citrate buffer−0.1 M $NaClO_4$ as supporting electrolyte. Scan rate was 0.1 V/s.

(D) Extensions to Other Core−Shell Structures. With the same basic approach as that described above, electrochemical techniques could also be used to characterize other metal−metal oxide core−shell structures and also bimetallic (metal-1@metal-2) core−shells.

In Scheme 2 we summarize the electrochemical detection of core−shell NPs in the case of bimetallic (Scheme 2A) and metal−metal oxide core−shell (Scheme 2B). When we have two metals X and Y NPs, Scheme 2A, the metal X could be oxidized (stripping) at potential E_X to produce X^+ and the metal Y could be oxidized at potential E_Y. The core−shell formed by X as core and Y as shell could be characterized by cyclic voltammetry. Two different cases are observed depending on the two potentials for oxidation. First when the potential E_X is less positive than E_Y, the first oxidation scan should show stripping at E_Y for both X and Y while no peaks corresponding to oxidation of metal X are observed at E_X because the metal Y shell isolates the core X. However, on the reverse (cathodic) scan, reduction peaks should be seen for the oxidized forms of X and Y, and when a second oxidation scan is carried out, stripping peaks of metal X are detected around E_X. This behavior demonstrates clearly the presence of core−shell structure. If the potential

Scheme 2. Electrochemical Characterization of Core−Shell NPs: (A) Bimetallic Core−Shell; (B) Metal Core/Metal Oxide Shell

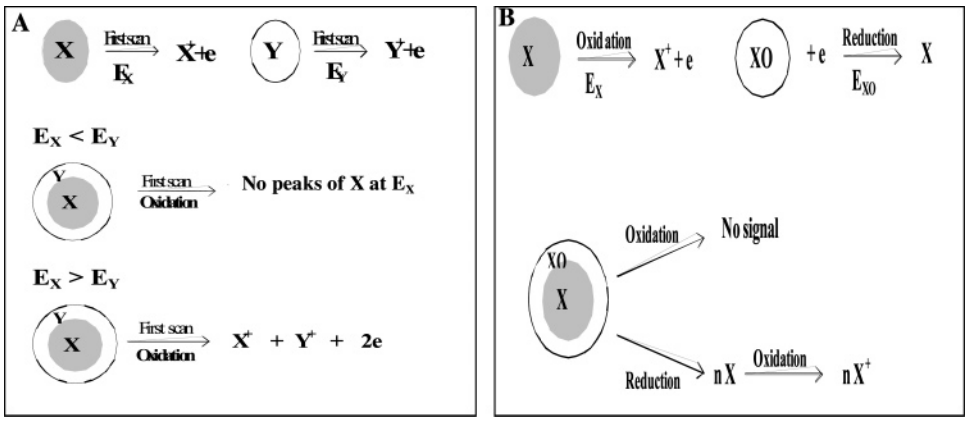

E_X is more positive than E_Y the first oxidation scan of the core−shell should exhibit two stripping peaks for both metal X and Y at their characteristic potentials. This latter behavior could not be clearly distinguished from a simple mixture of X and Y NPs.

Metal core (X) and its insulating (or reducible but not oxidizable) oxide (XO) shell could be also characterized using cyclic voltammetry as shown in Scheme 2B. Typically the metal X could be oxidized to form X^{n+} at potential E_X and the metal oxide XO could be reduced to form X at potential E_{XO} then reoxidized at E_X to form X^{n+}. Thus, the cyclic voltammetry of XO NPs shows reduction peaks (XO to X) followed by oxidation peak at reverse scan (X to X^+). It is important to notice that the charge efficiency, which represents the ratio between the anodic and cathodic charge for this experiment with a simple mixture of X and XO, is ~1. For the core−shell structure, X@XO, the first anodic scan does not show any stripping peaks (X to X^+) because the shell formed by XO protects the core X from oxidation. However, during a reduction scan a peak corresponding to reduction of XO is observed, and on the reverse scan, the oxidation stripping peak of X is detected. In this case the CE is much higher than 1, because of the additional available X formed after reduction of XO. The higher value of CE demonstrates clearly the presence of X@XO core−shell. In an analogous way NP with a metal oxide core and metal shell, XO@X, could be characterized electrochemically. In this case, beginning with a reduction scan, no peak is observed because the metal shell blocks the oxide reduction, but on an anodic scan stripping of X is observed. Following this, the second reduction scan should show a cathodic peak corresponding to reduction of a XO core. Additionally, Y@XO or YO@X core−shell might be characterized using cyclic voltammetry. These approaches assume that the shells are complete and do not allow electrochemistry of the core to occur because they block ion or solvent transfer from solution to the core. A closely related topic, e.g., the formation of a metallic silver shell around silver halide particles, has been recently described by Hasse et al., who have used atomic force microscopy (AFM) for the analysis of such systems. With AFM they could measure the thickness of the silver shell which has been formed by electrochemical reduction of solid silver halide particles on gold electrodes.[22]

Conclusion. The present work shows the facile manufacture of core−shell NPs, Ag@Ag_2O. Thus, the thermal treatment of Ag NPs, at temperature less than 360 °C and higher than 200 °C under air, leads to the formation of a thin layer of silver oxide over silver NPs. As a consequence core−shell structure Ag@Ag_2O is formed. Additionally, we have described a simple and effective electrochemical approach to characterize core−shell NPs. This technique is based on immobilizing the NPs in Nafion film onto a gold electrode. The evidence of the presence of core−shell NPs was studied using cyclic voltammetry. The absence of a stripping peak at the first oxidation scan demonstrates that the Ag_2O shell is blocking the electroactivity of the Ag core. However, after the reduction process, the silver oxide shell is reduced, and the reverse scan shows the stripping peak due to the oxidation of Ag. Moreover, the higher value of the charge efficiency, CE = 8, proves that the stripping observed is related to the oxidation of the silver core in addition to the silver formed after reduction of Ag_2O (normally for pure Ag_2O nanopatrticles CE = 0.9). Finally, the characterization of core−shell NPs using cyclic voltammetry could extend to different core−shell combinations such as bimetallic, metal oxide@metal, and metal@metal oxide.

Acknowledgment. The support of this work by NUCRYST Pharmaceuticals (Wakefield, MA) is gratefully acknowledged. We also thank Heechang Ye for taking TEM images and Dr. JiPing Zhou in TMI TEM facility at UT for helpful discussion.

References

(1) (a) Halperin, W. P. *Rev. Mod. Phys.* **1986**, *58*, 533. (b) Templeton, A. C.; Wuelfing, W. P.; Murray, R. W. *Acc. Chem. Res.* **2000**, *33*, 27. (c) Lam, D. M.-K.; Rossiter, B. W. *Sci. Am.* **1991**, *265*, 80. (d) Lewis, L. N. *Chem. Rev.* **1993**, *93*, 2693. (e) Murray, C. B.; Sun, S.; Doyle, H.; Betley, T. *Mater. Res. Soc. Bull.* **2001**, *26*, 985.

(2) (a) Novak, J. P.; Brousseau, L. C.; Vance, F. W.; Johnson, R. C.; Lemon, B. I.; Hupp, J. T.; Feldheim, D. L. *J. Am. Chem. Soc.* **2000**, *122*, 12029. (b) Murphy, C. J.; Jana, N. R. *Adv. Mater.* **2002**, *14*, 80. (c) Kim, F.; Song, J. H.; Yang, P. *J. Am. Chem. Soc.* **2002**, *124*, 14316. (d) Nicewarner-Peña, S. R.; Freeman, R. G.; Reiss, B. D.; He, L.; Peña, D. J.; Walton, I. D.; Cromer, R.; Keating, C. D.; Natan, M. J. *Science* **2001**, *294*, 137. (e) Ahmadi, T. S.; Wang, Z. L.; Green, T. C.; Henglein, A.; El-Sayed, M. A. *Science* **1996**, *272*, 1924. (f) Teng, X.; Black, D.; Watkins, N. J.; Gao, Y.; Yang, H. *Nano Lett.* **2003**, *3*, 261.

(3) (a) Chen, S.; Yang, Y. *J. Am. Chem. Soc.* **2002**, *124*, 5280. (b) El-Sayed, M. A. *Acc. Chem. Res.* **2001**, *34*, 257. (c) Maier, S. A.; Brongersma, M. L.; Kik, P. G.; Meltzer, S.; Requicha, A. A. G.; Atwater, H. A. *Adv. Mater.* **2001**, *13*, 1501. (d) Kamat, P. V. *J. Phys. Chem. B* **2002**, *106*, 7729.

(4) (a) Tkachenko, A. G.; Xie, H.; Coleman, D.; Glomm, W.; Ryan, J.; Anderson, M. F.; Franzen, S.; Feldheim, D. L. *J. Am. Chem. Soc.* **2003**, *125*, 4700. (b) Taton, T. A.; Mirkin, C. A.; Letsinger, R. L. *Science* **2000**, *289*, 1757. (c) Thanh, N. T. K.; Rosenzweig, Z. *Anal. Chem.* **2002**, *74*, 1624. (d) Kim, Y.; Johnson, R. C.; Hupp, J. T. *Nano Lett.* **2001**, *1*, 165. (e) Nath, N.; Chilkoti, A. *Anal. Chem.* **2002**, *74*, 504. (f) Roll, D.; Malicka, J.; Gryczynski, I.; Cryczynski, Z.; Lakowicz, J. R. *Anal. Chem.* **2003**, *75*, 3440.

(5) (a) Tessier, P. M.; Velev, O. D.; Kalambur, A. T.; Rabolt, J. F.; Lenhoff, A. M.; Kaler, E. W. *J. Am. Chem. Soc.* **2000**, *122*, 9554. (b) Nie, S.; Emory, S. R. *Science* **1997**, *275*, 1102. (c) Dick, L. A.; McFarland, A. D.; Haynes, C. L.; Van Duyne, R. P. *J. Phys. Chem. B* **2002**, *106*, 853. (d) Jackson, J. B.; Westcott, S. L.; Hirsch, L. R.; West, J. L.; Halas, N. J. *Appl. Phys. Lett.* **2003**, *82*, 257. (e) Sun, Y.; Xia, Y. *J. Am. Chem. Soc.* **2004**, *126*, 3892.

(6) (a) Pol, V. G.; Grisaru, H.; Gedanken, A. *Langmuir* **2005**, *21* (8), 3635. (b) Liz-Marzan, L. M.; Kamat, P. V. *Nanoscale Materials*; Kluwer Academic Publishers: Norwell, MA, 2003.

(7) Leslie-Pelecky, D. L.; Rieke, R. D. *Chem. Mater.* **1996**, *8*, 1770.

(8) (a) Toshima, N.; Yonezawa, T. *New J. Chem.* **1998**, *11*, 1179. (b) Caruso, F. *Adv. Mater.* **2001**, *13*, 11.

(9) Srnova-Sloufova, I.; Vlckova, B.; Bastl, Z.; Hasslett, T. L. *Langmuir* **2004**, *20* (8), 3407−3415.

(10) Shibata, T.; Bunker, B. A.; Zhang, Z.; Meisel, D.; Vardeman, C. F., II; Gezelter, J. D. *J. Am. Chem. Soc.* **2002**, *124* (40), 11989−11996.

(11) Toshima, N.; Harada, M.; Yamazaki, Y.; Asakura, K. *J. Phys. Chem.* **1992**, *96* (24), 9927−9933.

(12) Mizukoshi, Y.; Okitsu, K.; Maeda, Y.; Zamamoto, T. A.; Oshima, R.; Nagata, Y. *J. Phys. Chem. B* **1997**, *101* (36), 7033−7037.

(13) Schmid, G.; Lehnert, A.; Malm, J. O.; Bovin, J. O. *Angew. Chem., Int. Ed. Engl.* **1991**, *30* (7), 874−876.

(14) Mafuné, F.; Kohno, J.; Takeda, Y.; Kondow, T. *J. Am. Chem. Soc.* **2003**, *125* (7), 1686−1687.

(15) Sakai, T.; Alexandridis, P. *Chem. Mater.* **2006**, *18* (10), 2577−2583.

(16) Kim, H.; Achermann, M.; Balet, L. P.; Hollingsworth, J. A.; Klimov, V. I. *J. Am. Chem. Soc*. **2005**, *127* (2), 544−546.
(17) Lee, I. S.; Lee, N.; Park, J.; Kim, B. H.; Yi, Y.-W.; Kim, T.; Kim, T. K.; Lee, I. H.; Paik, S. R.; Hyeon, T. *J. Am. Chem. Soc*. **2006**, *128* (33), 10658−10659.
(18) Yang, J.; Lee, J. Y.; Chen, L. X.; Too, H.-P. *J. Phys. Chem. B* **2005**, *109* (12), 5468−5472.
(19) Ghilane, J.; Fan, F.-R. F.; Bard, A. J. Unpublished results.
(20) (a) L'vov, B. V. *Thermochim. Acta* **1999**, *333*, 13. (b) Dallek, S.; Parkhust, W. A.; Larrick, B. F. *Thermochim. Acta* **1984**, *78*, 333.
(21) Ghilane, J.; Hapiot, P.; Bard, A. J. *Anal. Chem*. **2006**, *78* (19), 6868−6872.
(22) Hasse, U.; Wagner, K.; Scholz, F. *J. Solid State Electrochem*. **2004**, *8* (10), 842−853.

NL070268P